International Journal of GEOMATE, May, 2026 Vol.30, Issue 141, pp.75-82
ISSN: 2186-2982 (P), 2186-2990 (O), Japan, DOI: https://doi.org/10.21660/2026.141.g13296
Geotechnique, Construction Materials and Environment

A FUNDAMENTAL STUDY ON FROST HEAVE AND THAW BEHAVIOR OF PILES AND FOUNDATIONS USED IN PHOTOVOLTAIC POWER GENERATION FACILITIES

Yusaku Fujita[1], *Dai Nakamura[2], Kenta Nakai[3], Takanori Kadota[4], Satsuki Kataoka[5], Yuki Minabe[6] and Takayuki Kawaguchi[7]

[1]Graduate School of Engineering, Kitami Institute of Technology, Japan;
[2, 4, 5, 6, 7]Faculty of Engineering, Kitami Institute of Technology, Japan;
[3]Asano Taiseikiso Engineering Co., Ltd, Japan

*Corresponding Author, Received: 05 May 2025, Revised: 01 Feb. 2026, Accepted: 05 Feb. 2026

ABSTRACT: In recent years, photovoltaic power generation facilities have been actively constructed in Hokkaido, Japan, a region characterized by a cold and snowy climate. However, considerable frost heave damage has been observed. In this study, a full-scale model experiment was conducted on piles and foundations used at photovoltaic power generation facilities to clarify their frost heave and thaw behavior. The experimental results show that the amount of frost heave decreases for both spiral piles and H-beam steel piles when the pile embedment depth is two to three times the maximum freezing depth. The results also indicate that, when the top surface of the footings is deeper than the freezing depth, the amount of frost heave of independent foundations becomes smaller. However, frost heave was observed in independent foundations with no footings or small footings. Based on these findings, effective frost heave countermeasures were examined and incorporated into the existing design guideline published in Japan.

Keywords: Frost heave, Spiral pile, H-beam steel pile, Independent foundation, Cold and snowy regions

1. INTRODUCTION

In recent years, global efforts toward decarbonization aimed at achieving net-zero greenhouse gas emissions have intensified, placing Japan under increasing pressure to transition from fossil fuels to renewable energy. Consequently, photovoltaic power generation facilities are being actively constructed even in Hokkaido, Japan, a region characterized by a cold and snowy climate. However, significant frost heave damage has been observed at these facilities.

Figure 1 shows examples of frost heave damage to solar panel mounts observed in eastern Hokkaido. Frost heave uplifts the foundations and piles supporting the solar panels, causing deformation of the mounts and subsequent warping of the panels. If such deformation progresses, the solar panels may tilt and eventually collapse. This type of damage is not unique to Japan and has also been reported in other cold and snowy regions, including Canada (e.g., Levasseur et al. [1]) and other parts of North America (e.g., Kibriya [2]).

In Japan, frost heave damage at photovoltaic power generation facilities primarily occurs because construction contractors lack reliable methods to predict and mitigate frost heave. Therefore, there is a strong need to develop effective frost heave countermeasures and corresponding design methods.

To address these issues, this study conducted an

Fig. 1 Examples of frost heave damage to solar panel mounts observed in eastern Hokkaido.

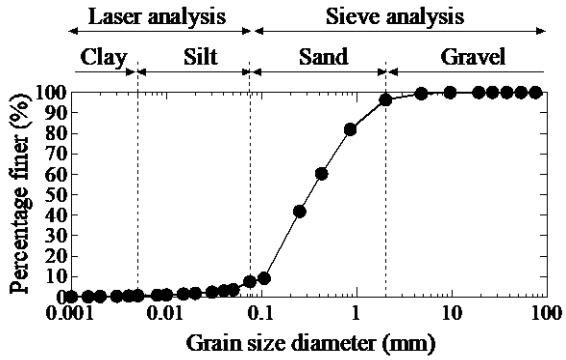

Fig. 2 Grain size cumulative distribution curve of the soil sample.

outdoor full-scale model experiment to clarify the frost heave and thaw behavior of piles and foundations used in photovoltaic power generation facilities. Subsequently, based on the findings, effective frost heave countermeasures were examined and incorporated into the existing design guideline published in Japan.

2. RESEARCH SIGNIFICANCE

This study evaluates the frost heave and thaw behavior of spiral piles, H-beam steel piles, and independent foundations through full-scale model experiments. Its significance lies in comparing the displacement characteristics of these foundations under natural freezing conditions. By investigating the effect of embedment depth on the amount of frost heave, this research provides empirical data to mitigate structural damage. These findings offer a practical basis for improving the reliability of photovoltaic facilities in seasonally frozen ground.

3. OVERVIEW OF THE FULL-SCALE MODEL EXPERIMENT

3.1 Soil Properties of the Experimental Site

In this study, full-scale models of piles and foundations were installed in ground consisting of sandy soil with high frost susceptibility. Various physical properties of the soil samples at the experimental site were measured using tests conducted in accordance with the Japanese Geotechnical Society Standards.

Figure 2 shows the grain size cumulative distribution curve of the soil sample obtained in accordance with the method stipulated by JIS A 1204 [3]. Based on the contents of coarse- and fine-grained fractions, the soil sample is classified as sand.

The soil particle density ρ_s is 2.51 g/cm^3, as determined in accordance with the method stipulated by JIS A 1202 [4].

Figure 3 shows the compaction curve of the soil sample obtained in accordance with the A-a method

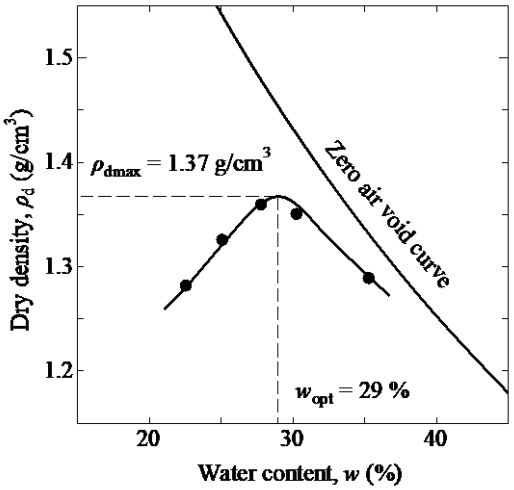

Fig. 3 Compaction curve of the soil sample.

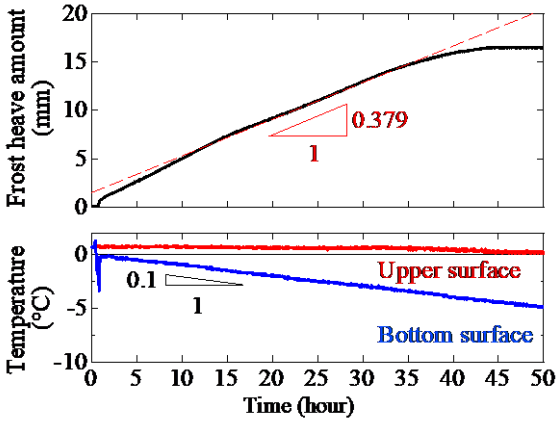

Fig. 4 Results of the frost heave test.

stipulated by JIS A 1210 [5] (the compaction energy E_c is 550 kJ/m^3 (standard Proctor)). The optimum water content w_{opt} is 29% and the maximum dry density ρ_{dmax} is 1.37 g/cm^3.

The dry density measured at the experimental site using a sampler with a volume 100 cm^3 was 1.22 g/cm^3 and the degree of compaction D_c was approximately 90%.

Figure 4 shows the results of the frost heave test conducted in accordance with the method stipulated by JGS 0172-2020 [6]. The frost heave rate obtained from the temporal variation in the frost heave amount is 0.379 mm/h. This value exceeds 0.3 mm/h, which is the threshold for high frost susceptibility according to the Japanese Geotechnical Society Standards.

3.2 Details of the Full-Scale Models

Table 1 summarizes the experimental conditions of this study. In this study, two types of piles (spiral piles and H-beam steel piles) and independent foundations were used as full-scale models. A total of nine experimental cases were conducted.

Figure 5 shows the appearance of the

Table 1 Experimental conditions of the study.

Case	Type of pile or foundation	Embedment depth (m)	Footing width (m)	Mass (kg)
1	Spiral pile	2.0	-	29
2	Spiral pile	1.5	-	23
3	Spiral pile	0.7	-	14
4	H-beam steel pile	2.0	-	35
5	H-beam steel pile	0.7	-	14
6	Independent foundation	0.7	0.25	380
7	Independent foundation	1.2	0.25	570
8	Independent foundation	1.2	0.10	460
9	Independent foundation	1.2	0.00	300

Fig. 5 Appearance of the experimental site.

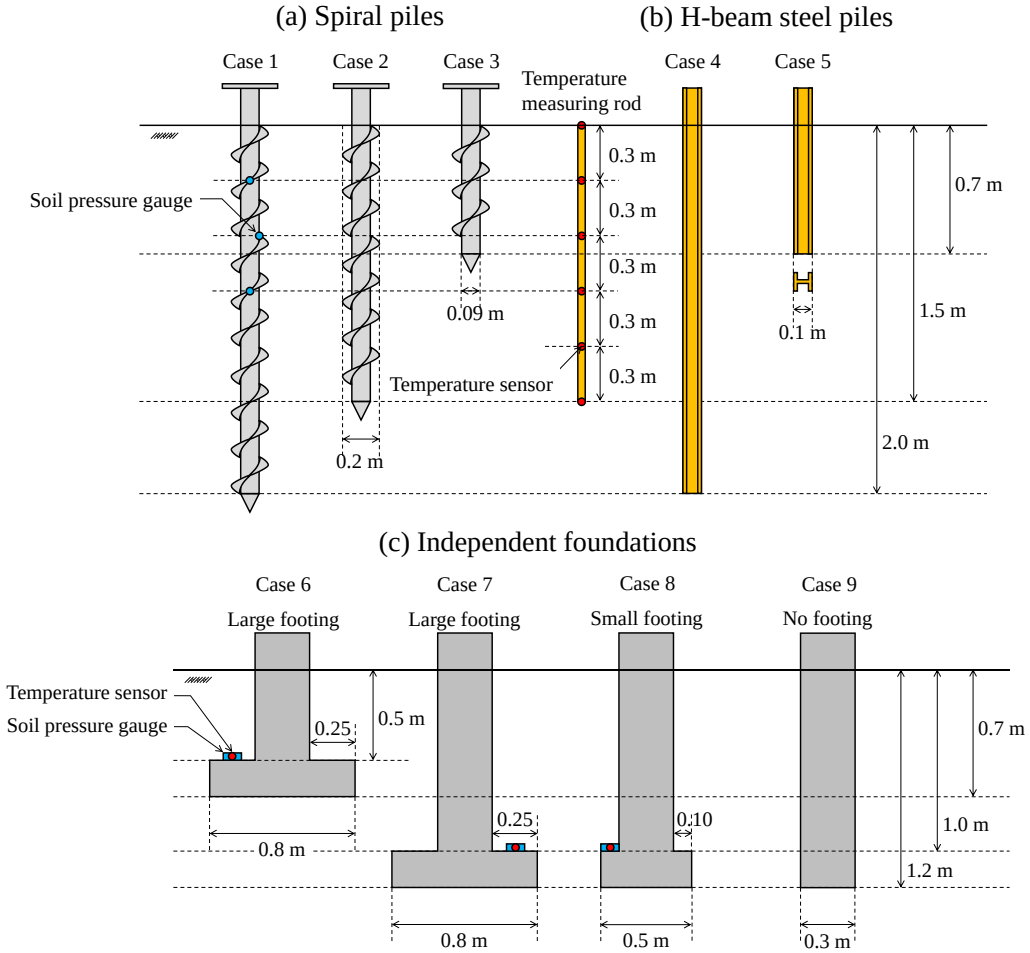

Fig. 6 Schematic diagram of (a) spiral piles, (b) H-beam steel piles, and (c) independent foundations installed in this study.

experimental site. In this study, the superstructure, including the solar panel and the mounting frame, was not installed. In addition, the area around the full-scale model was kept free of snow during the measurement period.

Figure 6 schematically illustrates the spiral piles, H-beam steel piles, and independent foundations that were installed, as well as the layout of various measuring instruments. Figure 7 shows examples of the spiral piles, H-beam steel piles, and independent foundations used in this study.

There are cases where the embedment depth is equal to the maximum freezing depth assumed for Kitami City (Case 3 with spiral piles, Case 5 with H-beam steel piles, and Case 6 with independent foundations). There are also cases where the

(a) Spiral pile (Case 1)

(b) H-beam steel pile (Case 4)

(c) Independent foundation (Case 7)

Fig. 7 Examples of the spiral piles, H-beam steel piles, and independent foundations used in this study.

(a) Spiral pile (Case 1)

(b) Independent foundation (Case 6)

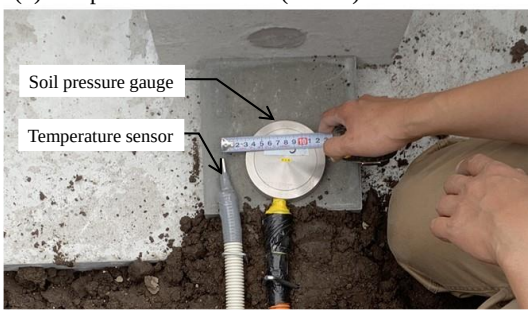

Fig. 8 Installation of soil pressure gauges on the spiral pile and independent foundations.

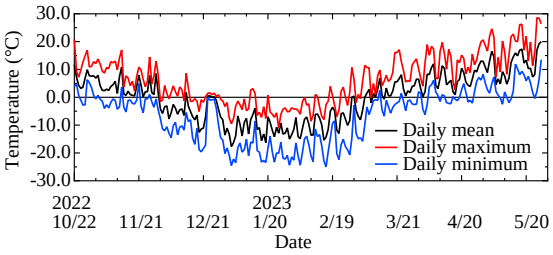

Fig. 9 Temporal variations in temperatures observed at AMeDAS Kitami.

embedment depth is greater than the maximum freezing depth (Cases 1 and 2 for spiral piles, Case 4 for H-beam steel piles, and Cases 7, 8, and 9 for independent foundations). The maximum freezing depth assumed in this study was set to 0.7 m.

As shown in Figure 6(c), there are cases with footings (Cases 6, 7, and 8) and without footings (Case 9) for independent foundations. In addition, there are cases with large footings (Cases 6 and 7) and with small footings (Case 8) for independent foundations.

The spiral piles with an embedment depth of 0.7 m and 1.5 m (Cases 2 and 3) were installed by rotary penetration, and the H-beam steel piles with an embedment depth of 0.7 m and 2.0 m (Cases 4 and 5) were installed by driving.

On the other hand, for the spiral pile with an embedment depth of 2.0 m (Case 1), the ground was excavated and then backfilled in order to install soil pressure gauges on the blades. All independent foundations (Cases 6 to 9) were constructed by backfilling after excavation.

3.3 Details of the Measurements

Figure 8 shows the installation of soil pressure gauges on spiral piles and independent foundations. The soil pressure gauges were embedded for the purpose of measuring the soil pressure applied to the upper surfaces of the blades of the spiral piles and the footings of the independent foundations. For independent foundations, temperature sensors were also installed in combination.

Temperature measurement rods were embedded for the purpose of measuring the freezing depth around the independent foundations and piles. The temperature sensors were installed at intervals of 0.3 m from the ground surface to a depth of 1.5 m. Soil pressures and soil temperatures were automatically measured at hourly intervals.

The amount of frost heave in winter and the amount of subsidence in spring in each case were observed through regular leveling surveys (approximately once every one to two weeks).

4. RESULTS AND DISCUSSIONS

4.1 Frost Heave and Thaw Behavior of Piles and Foundations

Figure 9 shows the temporal variations in temperatures observed at AMeDAS Kitami [7]. In 2022, Kitami City had a relatively cold winter, with

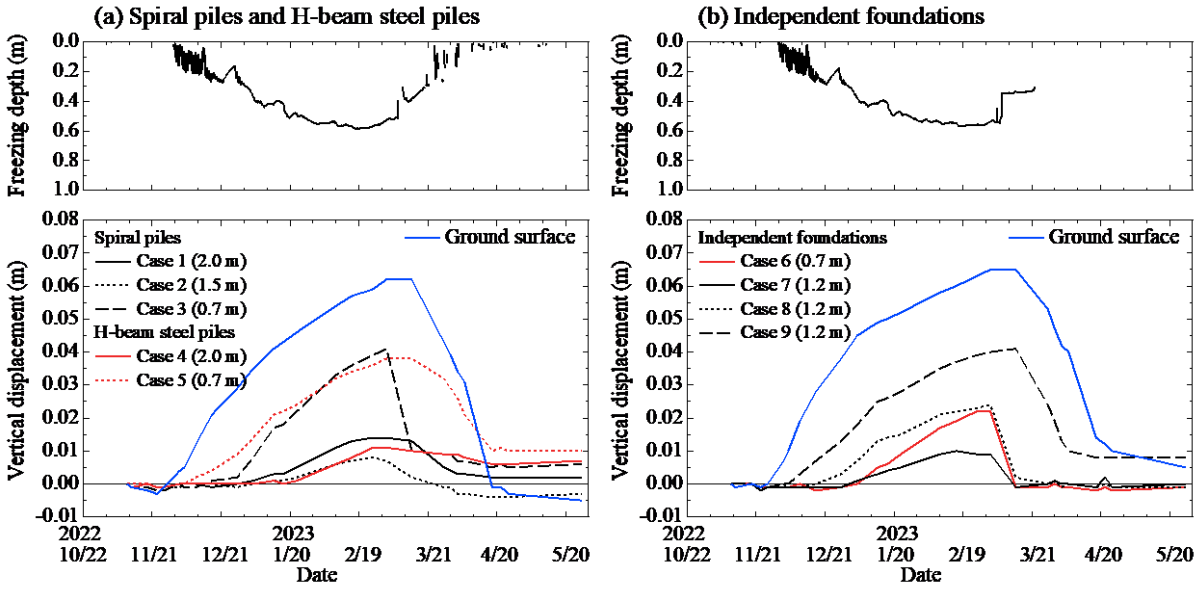

Fig. 10 Temporal variations of the freezing depth and vertical displacement of the spiral piles, H-beam steel piles, and independent foundations observed in this study.

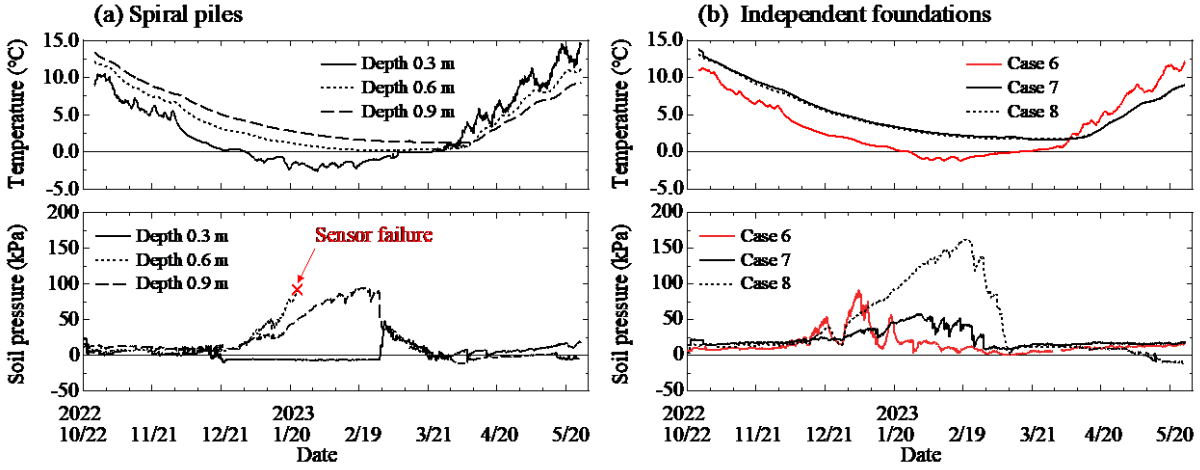

Fig. 11 Temporal variations of the soil pressure acting on the blades of the spiral piles and the footings of the independent foundations, as well as the soil temperatures.

the average daily temperature dropping below 0 °C from early December.

Figure 10 shows the temporal variations of the freezing depth and vertical displacement of the spiral piles, H-beam steel piles, and independent foundations.

In the freezing period shown in Figure 10(a), it was confirmed that the spiral pile (Case 3) and the H-beam steel pile (Case 5), which are shallowly buried, exhibited a large amount of frost heave. In contrast, both spiral piles (Cases 1 and 2) and the H-beam steel pile (Case 4), which are deeply buried, exhibited a small amount of frost heave. In the thawing period, the spiral pile exhibited greater subsidence and smaller residual displacement than the H-beam steel pile due to the soil pressure acting on the blades.

In the freezing period shown in Figure 10(b), it was confirmed that frost heave initiated in the foundation without footings (Case 9), followed by the foundation with small footings (Case 8) and the foundation with large footings (Case 7). In addition, even for foundations with large footings, those with shallower embedment depths (Case 6) began to exhibit frost heave earlier, and the final amount of frost heave was approximately double that of those with deeper embedment depths (Case 7). In the thawing period, the independent foundations rapidly returned to their original positions, partly owing to their large mass. However, only the foundation without footings (Case 9) did not return to its original position and exhibited residual displacement.

Figure 11 shows the temporal variations of the soil pressure acting on the blades of the spiral pile and the footing of the independent foundation, as well as the soil temperatures.

From the soil pressure gauges installed on the

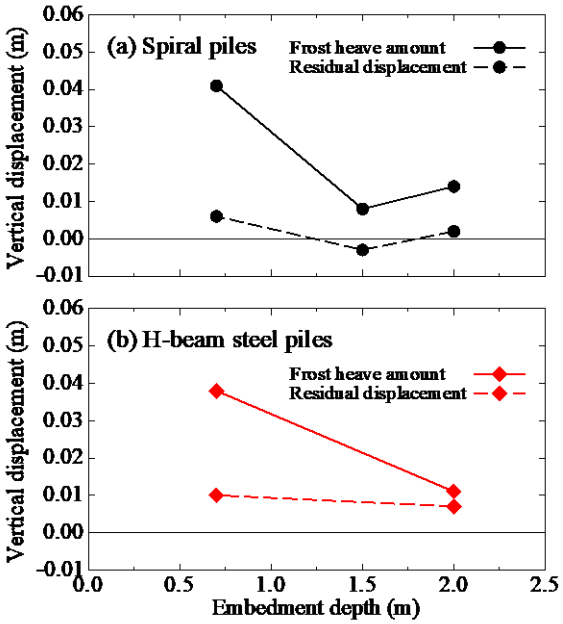

Fig. 12 Relationships between pile embedment depth and the amounts of frost heave and residual displacement.

blades of the spiral pile (Case 1) in Figure 11(a), the soil pressure at an embedment depth of 0.3 m became negative when the temperature reached 0 °C. On the other hand, the soil pressures at embedment depths of 0.6 m and 0.9 m continued to increase as the temperature decreased. In addition, the soil pressure at an embedment depth of 0.6 m was greater than that at an embedment depth of 0.9 m. This is considered to be due to the soil pressure and frost heave pressure acting on the blades. However, owing to instrument failure, the soil pressure at the embedment depth of 0.6 m was not measured after the end of January.

From the soil pressure gauges installed on the footings of the independent foundations (Cases 6, 7, and 8) in Figure 11(b), for foundations with an embedment depth of 1.2 m, it was confirmed that the soil pressure was higher in the foundation with small footings (Case 8) than in the foundation with large footings (Case 7), because the amount of frost heave was greater. In addition, for the foundation with large footings and a shallow embedment depth (Case 6), the soil pressure increased markedly at the early stage of the freezing period. However, when the freezing depth reached the top of the footings (0.5 m), the soil pressure decreased significantly.

4.2 Effects of Pile Embedment Depth and Footing Width of Independent Foundations on Frost Heave and Residual Displacement

Figure 12 shows the relationships between the pile embedment depth and the amounts of frost heave and residual displacement. The amount of frost heave and the amount of residual displacement decreased as the piles were buried deeper.

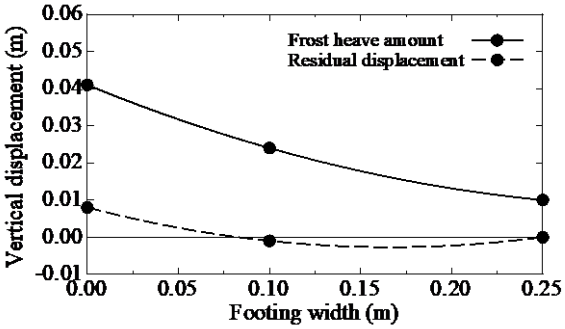

Fig. 13 Relationship between the footing width of the independent foundation and the amounts of frost heave and residual displacement.

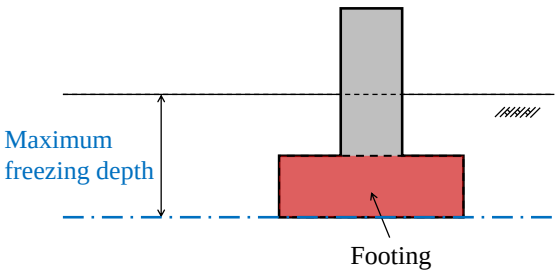

Fig. 14 Continuous foundation embedment method presented in the Design Guideline for Ground-Mounted Photovoltaic Power Generation Systems (2019 Edition) [8].

Figure 13 shows the relationship between the footing width of the independent foundation and the amounts of frost heave and residual displacement. The amount of frost heave and the amount of residual displacement decreased as the footing width of the independent foundations increased.

5. PROPOSED DESIGN GUIDELINE

5.1 Existing Design Guideline Published in Japan and Its Issues

At the time this study was initiated, the Design Guideline for Ground-Mounted Photovoltaic Power Generation Systems (2019 Edition) [8] had been published by the New Energy and Industrial Technology Development Organization (NEDO). This guideline is useful for applications in warm regions; however, the countermeasures for cold and snowy regions are insufficient. In particular, the embedment depth for continuous foundations specified in the guideline is not appropriate as a frost heave countermeasure. In addition, the guideline does not provide any specific frost heave countermeasures for piles.

Figure 14 illustrates the continuous foundation embedment method presented in the guideline. The guideline recommends setting the embedment depth such that the bottom of the footing reaches the

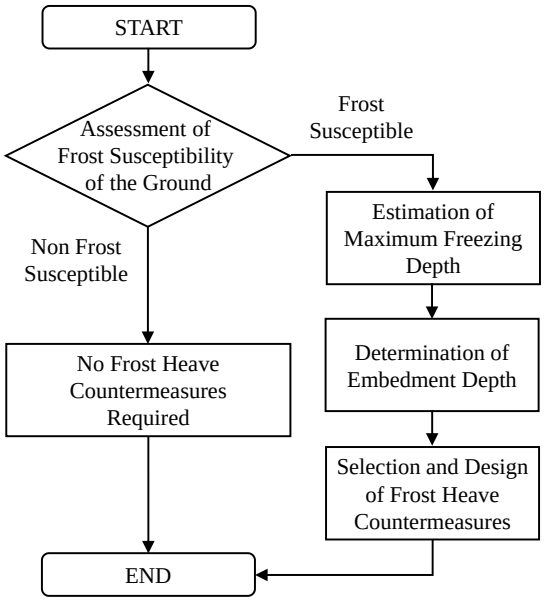

Fig. 15 Flowchart for the examination of frost heave countermeasures for photovoltaic power generation facilities.

maximum freezing depth. However, when compared with the findings of this study, this embedment method is considered to have a high potential for frost heave occurrence. As a result, inappropriate design practices may have been widely disseminated among construction contractors.

5.2 Frost Heave Countermeasures Added to the Design Guideline

The results of this study have been incorporated as frost heave countermeasures in the Design Guideline for Ground-Mounted Photovoltaic Power Generation Systems, revised in 2025 [9].

5.2.1 Flowchart for the examination of frost heave countermeasures for photovoltaic power generation facilities

Figure 15 shows a flowchart for the examination of frost heave countermeasures for photovoltaic power generation facilities.

First, ground investigations are conducted to confirm whether the soil within the range affected by freezing (i.e., above the maximum freezing depth) is frost susceptible. For evaluating the frost susceptibility of in-situ soil, the Japanese Geotechnical Society Standard, “Test method for frost susceptibility of soils (JGS 0172-2020)” [6], is recommended, as it enables a direct assessment of frost susceptibility.

Next, the freezing depth is estimated. The freezing depth is defined as the maximum depth from the ground surface before freezing to the depth at which the ground temperature reaches 0 °C. The theoretical maximum freezing depth is calculated by first

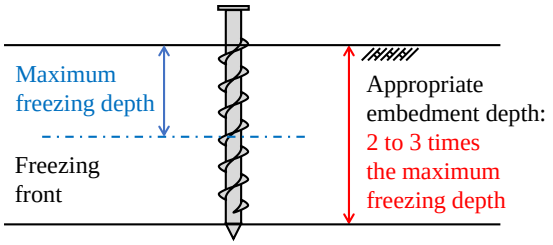

Fig. 16 Appropriate embedment method for spiral piles.

determining the freezing index F from meteorological data obtained at the AMeDAS station closest to the site. The freezing depth corresponding to F is then estimated using the following equation, which is a simplified form of the modified Berggren equation proposed by Aldrich [10]. The freezing index is defined as the absolute value of the cumulative daily mean air temperature during the period in which the daily mean temperature continuously remains below 0 °C.

$$D_{max}=C\sqrt{F} \quad \textbf{(1)}$$

where D_{max} denotes the theoretical maximum freezing depth (cm), F represents the freezing index used for design (°C·days), and C is the freezing coefficient. In addition, the freezing coefficient C is empirically known to fall within the range of $2 \leq C \leq 4$.

5.2.2 Frost Heave Countermeasures

In cold and snowy regions, when the ground consists of frost susceptible soils, it is necessary either to implement a soil replacement method in which the soil is replaced with non-frost susceptible soil down to the freezing depth, or to apply frost heave countermeasures.

Using spiral piles as foundations is effective as a frost heave countermeasure. This is because soil pressure acts on the upper surface of the blades, thereby restraining upward vertical displacement caused by frost heave.

Figure 16 illustrates the appropriate embedment method for spiral piles. Experimental results indicate that embedding spiral piles to a depth approximately 2 to 3 times the maximum freezing depth is highly effective as a frost heave countermeasure. Conversely, if the embedment depth is shallower than the maximum freezing depth, even spiral piles cannot provide sufficient mitigation. Furthermore, cylindrical piles without blades, H-beam steel piles, or screw piles with small blades can also reduce frost heave displacement if they are buried to an appropriate depth.

Similarly, using independent foundations or continuous foundations is also effective. Soil pressure acting on the upper surface of the footing helps restrain upward vertical displacement. However, since frost heave may occur once the freezing front

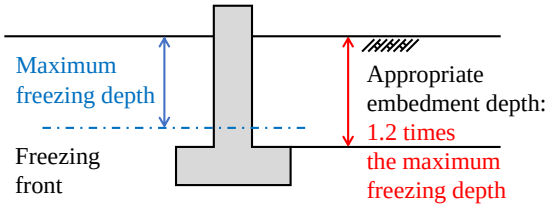

Fig. 17 Appropriate embedment method for independent foundations and continuous foundations.

reaches the upper surface of the footing, the top surface of the footing should be buried deeper than the maximum freezing depth. In addition, the footing width should be sufficiently large to ensure that soil pressure can effectively act on it.

Figure 17 illustrates the appropriate embedment method for independent foundations and continuous foundations. Based on experimental results, frost heave can be prevented by setting the embedment depth (from the ground surface to the top surface of the footing) to be approximately 1.2 times the predicted maximum freezing depth. However, if the ground at the site exhibits extremely high frost susceptibility, or if the superstructure cannot tolerate frost heave displacement, it is also advisable to consider frost heave countermeasures that combine these foundations insulation or soil replacement methods.

6. CONCLUSION

In this study, a full-scale model experiment was conducted on piles and foundations used in the construction of photovoltaic power generation facilities to clarify their frost heave and thaw behavior.

The experimental results confirm that the amount of frost heave decreases for both spiral piles and H-shaped steel piles when the pile embedment depth is two to three times the freezing depth. They also confirm that when the top surface of the footings is deeper than the freezing depth, the amount of frost heave of the independent foundation becomes smaller. However, frost heave occurs in independent foundations with no footings or with small footings.

The results of this study have been incorporated as frost heave countermeasures in the Design Guideline for Ground-Mounted Photovoltaic Power Generation Systems, revised in 2025.

The findings obtained in this study contribute not only to the advancement of design and construction technologies for photovoltaic systems but also to the safe and stable expansion of renewable energy deployment in cold and snowy regions.

7. ACKNOWLEDGMENTS

These findings were obtained as a result of work commissioned by the New Energy and Industrial Technology Development Organization (NEDO), a national research and development agency.

8. REFERENCES

1. Levasseur. P., Maher. M. L. J. and Dittrich. J. P. A case study of frost action on lightly loaded piles at Ontario solar farms, in Proc. Int. Conf. GeoQuebec, 2015, pp. 1-7.
2. Kibriya. T. Rehabilitation techniques to address frost effects on pile foundations of solar power generation facilities in north America, International Journal of Applied Engineering Research, Vol. 13, No. 10, 2018, pp. 7333-7339.
3. Japanese Industrial Standards (JIS), JIS A 1204:2020, Test method for particle size distribution of soils, Japanese Standards Association, 2020.
4. Japanese Industrial Standards (JIS), JIS A 1202:2020, Test method for density of soil particles, Japanese Standards Association, 2020.
5. Japanese Industrial Standards (JIS), JIS A 1210:2020, Test method for soil compaction using a rammer, Japanese Standards Association, 2020.
6. Japanese Geotechnical Society (JGS), JGS 0172-2020, Test method for frost susceptibility of soils, Japanese Geotechnical Society, 2020.
7. Japan Meteorological Agency, http://www.data.jma.go.jp/obd/stats/etrn/index.php
8. New Energy and Industrial Technology Development Organization (NEDO), Design Guideline for Ground-Mounted Photovoltaic Power Generation Systems (2019 Edition), Kawasaki, Kanagawa, Japan: NEDO, 2019, pp. 1-122 (in Japanese). https://www.nedo.go.jp/content/100895022.pdf
9. New Energy and Industrial Technology Development Organization (NEDO), Design Guideline for Ground-Mounted Photovoltaic Power Generation Systems (2025 Edition), Kawasaki, Kanagawa, Japan: NEDO, 2025, pp. 1–188 (in Japanese). https://www.nedo.go.jp/content/800023895.pdf
10. Aldrich. H. D. J. Frost penetration below high way and airfield pavement, Highway Research Board, Bulletin, Vol. 135, 1956, pp. 124-149.